MASTER'S DEGREE THESIS

Master of Science in Advanced Mathematics and Mathematical Engineering

Title: Comparison of a size-dependent model for the latent heat of small tin nanoparticles

Author: Adrià González Esteve

Advisor: Tim Myers

Department: Matemàtiques

Academic year: 2015-2016

UNIVERSITAT POLITÈCNICA DE CATALUNYA
BARCELONATECH
Facultat de Matemàtiques i Estadística

Universitat Politècnica de Catalunya
Facultat de Matemàtiques i Estadística

Master in Advanced Mathematics and Mathematical Engineering

Master's Thesis

Correction of a size-dependent model for the latent heat of small tin nanoparticles

Adrià González Esteve

Supervised by Tim Myers
Departament de Matemàtiques
June, 2016

A un arbre ple de mandarines.

Abstract

Keywords: Classical thermodynamics, Stefan problem, Moving phase change boundary, Boundary condition, Melting point depression, Perturbed solution

MSC2010: 80A22, 74N20

The classical formulation for the Stefan problem at the nanoscale does not work because the melting temperature and the effective latent heat decrease with the nanoparticle size. In this work, a model for the effective latent heat is corrected because it does not correspond to the definition of latent heat. This model is used to see the consequences of imposing a Dirichlet boundary condition instead of a convective boundary condition. To do it, the liquid and the solid problem are simplified using a perturbed solution to reduce the Stefan problem into a first order ODE.

Contents

Chapter 1

Introduction

1.1 Motivation

The Stefan problem is a classical moving boundary problem for the phase change. Its study implies a formulation of the interface movement due to the energy conservation through the internal boundary, the problem is that the classical formulation does not work at the nanoscale. The increase of the surface-to-volume ratio makes the thermodynamics and some thermal properties change. For this reason, there is an industrial interest in its study.
At the macroscale, lots of properties of the materials are taken as constants, like the melting temperature ($T_m^\star$) or the latent heat of fusion ($L_m^\star$), among other properties. These properties are represented with a $\star$ because they correspond to the bulk value, the expected value for a material. But experiments show that these properties change with nanoparticles size. Buffat and Borel [4] reported a decrease of approximately 500 K below the bulk melt temperature (approximately 60%) for gold nanoparticles with radii a little above 1 nm [12]. This phenomenon is known as the melting point depression.
In the case of latent heat of fusion, Lai *et al.* found a reduction up to 70% from the bulk latent heat for tin (Sn) nanoparticles of 5 nm in diameter [12]. The problem of Lai *et al.* data is that it does not correspond to the definition of latent heat, so it cannot be used in models for nanoparticle melting. The data from Lai *et al.* corresponds to the energy needed for the whole melting given an initial radius, not to the energy absorbed instantaneously during melting for a nanoparticle size. For this reason, a correction of the data from Lai *et al.* is introduced in this work.
Melting point depression, applied to the latent heat, was considered in [8, 9] but in both studies the outer boundary temperature was taken as a constant [12], a surrounding temperature greater than the bulk melt temperature ($T_H > T_m^\star$). This assumption is usually taken for mathematical convenience also at the macroscale, not only at the nanoscale. Fixing a heat temperature implies an infinite heat transfer from the heating source that physically is unrealistic and will make the melting faster. For this reason, a Newton cooling condition is going to be used instead of a Dirichlet boundary condition. In

other words, a heat flux proportional to the difference with the surrounding temperature $q_H = \alpha\,(T_H - T)$, where α is the heat transfer coefficient. Using this expression, the Dirichlet boundary condition can be recovered taking $\alpha \to \infty$. This Robin condition was used in Ribera and Myers [12] but, unlike them, in this work the velocity of the liquid is going to be neglected, which means that the convective terms of the heat equation will not be taken into account.
In order to study the consequences of imposing a Robin boundary condition or a Dirichlet boundary condition, the solid and the liquid problem are going to be simplified using a perturbed solution to reduce the problem to a simpler ODE. The perturbation method is to approximate a solution by a power series in a small parameter ε [5]. For the solid problem is going to be used that the thermal conductivity of the solid is really large compared to the thermal conductivity of the liquid, then the small parameter for the solid will be $\varepsilon := k_l/k_s \ll 1$. For the liquid problem, is going to be considered that during melting the latent heat is larger than the sensible heat, so the heat equation can be considered as a steady-state problem compared to the movement of the boundary. Then the small parameter for the liquid will be the Stefan number $\varepsilon := \mathrm{St} \ll 1$. The Stefan number (St) is defined as the ratio of sensible heat to latent heat, whose inverse is $\beta = 1/\mathrm{St}$.
Then the structure of this work will be the following:

- In the next Section, the Stefan condition at the nanoscale is going to be introduced, treating the liquid as a solid.
- In Chapter 2 is going to be discussed the size dependency of the melt temperature and the latent heat of fusion.
- In Chapter 3, the Stefan problem is going to be reduced to the liquid phase. For the solid problem a perturbed solution is going to used taking $1/k$ as small parameter.
- In Chapter 4 an ODE for the Stefan problem is going to be obtained. The temperature in the liquid will be approximated using a perturbed solution where a Robin boundary condition is going to be imposed.
- In Chapter 4 also, the two outer boundary conditions are going to be compared.
- Finally, in Chapter 5, the melting times are going to be computed for all these different situations.

1.2 Stefan condition at the nanoscale

The Stefan condition, as said in the previous Section, comes from the energy conservation through the internal boundary during melting. The first law of classical thermodynamics states that the difference in internal energy of a closed system is equal to the amount of heat added to the system and the work done on the system [3]. As it is said before, the liquid motion is going to be neglected $\mathbf{v} = 0$, then the heat is going to be transmitted by conduction and there is no work done by pressure forces and viscous forces because there is no fluid.

$$\frac{\partial}{\partial t}(\rho u) + \nabla \cdot \mathbf{q} = 0, \tag{1.1}$$

where u is the specific internal energy, ρ is density and $\mathbf{q}$ is the heat flux. As it is observed in equation (1.1) there is no kinetic nor convective term in the energy conservation equation like in [12]. As in Bird *et al.* [3] it is convenient to switch from the internal energy to enthalpy using the definition of specific enthalpy, $h = u + p/\rho$. Then the conservation equation (1.1) becomes

$$\frac{\partial}{\partial t}(\rho\, h - p) + \nabla \cdot \mathbf{q} = 0, \tag{1.2}$$

where p is pressure. From this conservation equation, the Stefan condition can be obtained using the Rankine-Hugoniot condition [6, 2]. The Rankine-Hugoniot condition, from a conservation law, ensures conservation across a moving surface.

$$\frac{\partial}{\partial t}F + \nabla \cdot \mathbf{G} = 0 \Rightarrow [F]^{+}_{-}\, s_t = [\mathbf{G} \cdot \mathbf{n}]^{+}_{-}\,, \tag{1.3}$$

where $[\,\cdot\,]^{+}_{-}$ is the jump across the discontinuity surface and $s_t = \mathbf{s_t} \cdot \mathbf{n}$ is the speed of the moving boundary. In this case, the $+$ superscript indicates the fluid and the $-$ the solid. But before applying the Rankine-Hugoniot to the conservation of energy, it is going to be applied first to the mass conservation equation. It is obtained

$$\frac{\partial}{\partial t}\rho + \nabla \cdot (\rho \mathbf{v}) = 0 \Rightarrow [\rho]^{+}_{-}\, s_t = 0, \tag{1.4}$$

because in this study has been considered that $\mathbf{v} = 0$. This means that there is no density jump through the interface and the liquid that appears has the same density as the solid that melts, $\rho_l = \rho_s$. If it had been a solidification study, ρ_l should be considered as the density at the interface. Now applying the Rankine-Hugoniot condition (1.3) to the energy conservation equation (1.2), the Stefan condition is

$$\left([\rho h]^{+}_{-} - [p]^{+}_{-}\right) s_t = [\mathbf{q} \cdot \mathbf{n}]^{+}_{-}\,, \tag{1.5}$$

where $[\rho h]^{+}_{-} = \rho_s\, [h]^{+}_{-} = \rho_s L_m(t)$ by definition of latent heat, $[p]^{+}_{-} = -2\kappa\sigma^{\star}_{sl}$ according to Young-Laplace equation and $\mathbf{q} \cdot \mathbf{n} = -k\nabla T$ using Fourier's law.

κ corresponds to the mean curvature of the interface surface and $\sigma_{sl}^{\star}$ is the bulk surface energy between the solid and the liquid. Recovering the Stefan condition, its expression is

$$\left(\rho_s L_m(t) + 2\kappa\sigma_{sl}^{\star}\right) s_t = k_s \nabla\theta \cdot \mathbf{n}\Big|_{x=s} - k_l \nabla T \cdot \mathbf{n}\Big|_{x=s}, \tag{1.6}$$

where k is heat conductivity (subscripts s and l denote solid and liquid), T is the liquid temperature and θ is the solid temperature. This Stefan condition is different to the usual formulation because of the surface tension term. At the mascroscale the curvature of the interface is insignificant so this term would be neglected. But at the nanoscale cannot be neglected because the curvature is of the order $\kappa \sim 1/R$, where R is the radius of the nanoparticle. This new Stefan condition (1.6) involves an effective latent heat [12], which in this study is the sum of the size dependent latent heat and the energy required to create the new surface during melting.

$$L_m^{\text{eff}}(R) = L_m(R) + 2\kappa(R)\frac{\sigma_{sl}^{\star}}{\rho_s}. \tag{1.7}$$

However, this material property is usually taken as a constant, like in the macroscale, taking the bulk value of the latent heat. For this reason, in the next Chapter is going to be discussed the size dependency of the melting temperature and the latent heat of fusion.

Chapter 2

Size-dependent melting properties

As said in the Introduction, at the nanoscale, there are some properties that change with nanoparticle size. Some experiments show that the melting temperature and the latent heat of melting are not constant during melting. The melting point depression is a well-known phenomenon but for the latent heat is not the case. In this work is going to be introduced a model for latent heat of fusion using the model proposed by Ribera and Myers [12] but correcting the data from Lai *et al.* [10] from which they rely.

2.1 Melting point depression

From experiments, it has been observed that the melting temperature decreases with size at the nanoscale. The temperature where melting takes place is not the bulk value anymore.

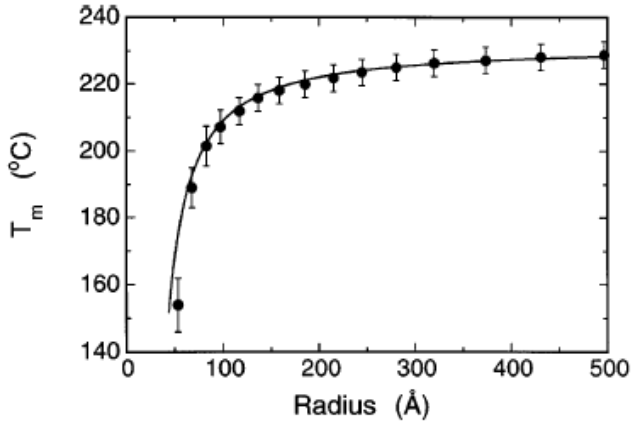

Figure 2.1: Size dependence of the melting points of Sn particles. The solid line corresponds to the model proposed by Lai *et al.*. Taken from [10].

For this reason, the Gibbs-Thomson relation is typically used for the melting temperature [2, 8, 11]

$$T_m = T_m^\star \left[1 - \frac{2\kappa\sigma_{sl}^\star}{\rho_s L_m^\star}\right]. \tag{2.1}$$

This equation (2.1) explains how the melt temperature decreases as the curvature at the interface increases [7]. At the mascroscale, $\kappa\sigma_{sl}^\star \ll \rho_s L_m^\star$, so the melting temperature corresponds to the bulk value.
In this study is going to be studied the melting of spherical nanoparticles, then the mean curvature of the interface corresponds to $\kappa = 1/R$. As the size of the nanopaticle changes during melting, the melting temperature also depends on time.

2.2 Latent heat variation

Despite the widespread use of the Gibbs-Thomson relation for the melting point depression, the latent heat of fusion is usually considered as a constant taking its bulk value. Some papers have tried to introduce this variation taking advantage of melting point depression [2, 7, 11, 8] using this model

$$L_m^{MD} = L_m^\star + (c_l - c_s)\,(T_m - T_m^\star)\,, \tag{2.2}$$

where c is the specific heat. In this case, the second term of the effective latent heat corresponds to the decreasing related to the melting point depression. The problem of this expression is that is commonly assumed $c_s \simeq c_l$ [11], that makes this reduction insignificant. But in Figure 2.2 it is observed that the decreasing of the effective latent heat is considerable.

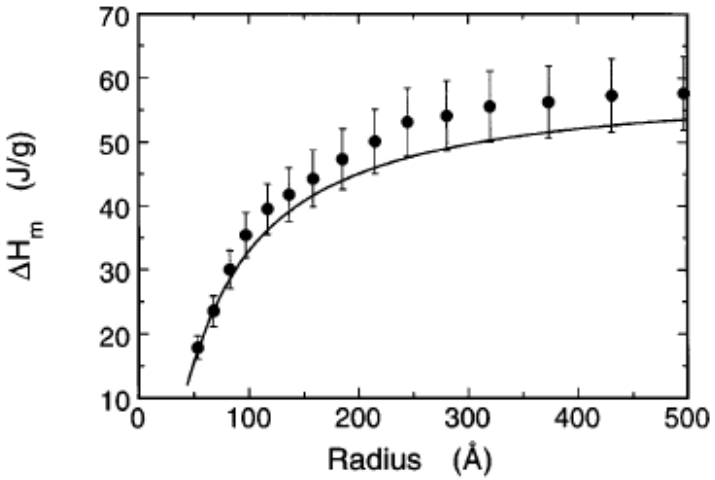

Figure 2.2: Size dependence of the normalized heat of fusion of tin nanoparticles, taken from [10]. The solid line is the expression proposed by Lai *et al.*

For this reason, Ribera and Myers proposed an exponential model.

$$L_m^{RM} = L_m^\star \left(1 - e^{-C\frac{R}{R_C}}\right), \tag{2.3}$$

where $R_C = \sigma_{sl}^\star / \rho_s L_m^\star$ is the capillary length and the constant C is a fitting parameter. It is obtained via a least-squares fit to the data in Figure 2.2 [12]. Using the thermodynamical data for tin in Table 2.1 the fitting parameter corresponds to $C = 0,0133$ according to Ribera and Myers [12].

Material	$L_m^\star$ [J/kg]	ρ_s [kg/m^3]	$\sigma_{sl}^\star$ [N/m]
Tin	58500	7180	0,064

Table 2.1: Tin properties, taken from Ribera and Myers [12].

The problem of this model is that the data from Lai *et al.* does not correspond to the definition of latent heat. The latent heat is defined as the energy absorbed by a unit mass at its melting point and it has been shown in Section 2.1 that this point changes with time. Then, integrating the energy delivered during melting and dividing it by the initial mass does not correspond to the definition of latent heat. This will be discussed in the next Section.

2.3 Correction of Lai data

In the previous Section 2.2 it has been noticed in Figure 2.2 that the latent heat of fusion depends on the nanoparticle size, from the data obtained by Lai *et al.* [10]. The problem is that the measure that they related to the effective latent heat does not correspond to the definition of effective latent heat. To visualize this error, their experiments are going to be explained, to deduce how to correct these measures.

The first step is to generate the nanoparticles but controlling its size because it is interesting to get the dependency of the measurements with size. To achieve this goal, Lai *et al.* used thermal evaporation, this technique consists on heating a material in a vacuum chamber until its surface atoms have sufficient energy to leave the surface [1]. This method allows to obtain nanoparticles of Sn whose radius depends on the duration of the deposition (~ 3 Å/s). Nevertheless, to get exactly the size of the nanoparticles in every experiment, Lai *et al.* [10] used a scanning electron microscope.

Once the nanoparticles are generated, it is time for the melting using a calorimeter to measure some variables. In this case it is important to monitor the current and the voltage delivered to the calorimeter to obtain the melting temperature and the power delivered during melting. Integrating this power, the heat provided to the nanoparticles can be recovered. But the sensible heat needed to reach the melting temperature must be subtracted to obtain the heat related to the melting. In Figure 2.3 it can be observed, that during melting there is an abrupt change of the energy delivered to the calorimter.

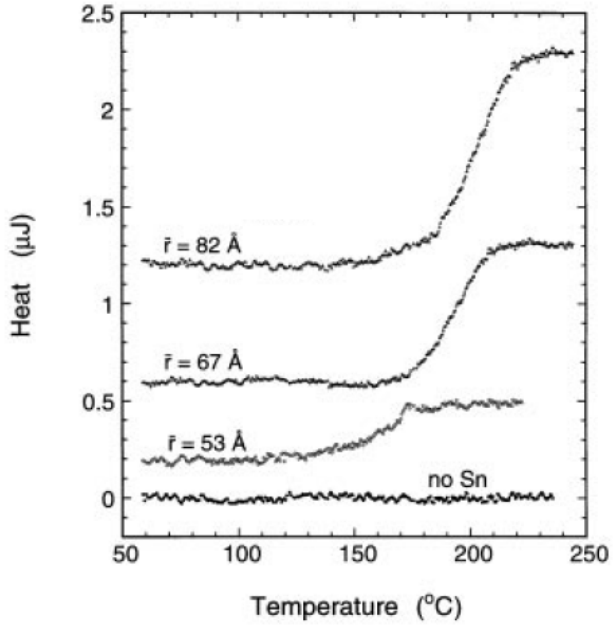

Figure 2.3: Heat measures for different radii, taken from Lai *et al.* [10].

Lai *et al.* took this heat jump as a measure of L_m^{eff} and it can be observed in Figure 2.3 that it decreases with the nanoparticle size. So the melting becomes easier once it has started and less energy is needed for the phase change. Then the real $\bar{L}_m^{\text{eff}}$ that Lai *et al.* [10] measures correspond to this mapping

$$\frac{\text{Energy}}{m_0} = \frac{\int_0^{m_0} L_m^{\text{eff}}(m)\, dm}{m_0} \longmapsto \bar{L}_m^{\text{eff}}(m_0) \equiv \bar{L}_m^{\text{eff}}(R_0), \tag{2.4}$$

if it is considered that the effective latent heat depends on mass. But using the fact that effective latent heat decreases during melting, it is easy to get

$$\bar{L}_m^{\text{eff}}(m_0) := \frac{\int_0^{m_0} L_m^{\text{eff}}(m)\, dm}{m_0} < \frac{\int_0^{m_0} L_m^{\text{eff}}(m_0)\, dm}{m_0} = L_m^{\text{eff}}(m_0), \tag{2.5}$$

this means that the measure that Lai *et al.* related to the effective latent heat, is lower than its definition. However, the definition of effective latent heat can be recovered if it is obtained a relation with the mapping done in (2.4). Recovering the dependence with size, the mapping corresponds to

$$\bar{L}_m^{\text{eff}}(R) = \frac{\int_0^R L_m^{\text{eff}}(r)\, \rho\, 4\pi r^2\, dr}{\rho\, \frac{4}{3}\pi R^3} = \frac{3}{R^3}\int_0^R L_m^{\text{eff}}(r)\, r^2\, dr. \tag{2.6}$$

Rearranging

$$\frac{R^3 \bar{L}_m^{\text{eff}}(R)}{3} = \int_0^R L_m^{\text{eff}}(r)\, r^2\, dr. \tag{2.7}$$

This expression can be derived using the fundamental theorem of calculus

$$R^2 \bar{L}_m^{\text{eff}}(R) + \frac{R^3 \bar{L}_m'^{\text{eff}}(R)}{3} = L_m^{\text{eff}}(R)\, R^2. \tag{2.8}$$

Then, the definition of effective latent heat is related to Lai *et al.* mapping using the expression

$$L_m^{\text{eff}}(R) = \bar{L}_m^{\text{eff}}(R) + \frac{R}{3} \bar{L}_m'^{\text{eff}}(R), \tag{2.9}$$

that is clearly bigger than the mapping that Lai *et al.* [10] did because $\bar{L}_m'^{\text{eff}}(R)$ is positive (see Figure 2.2). The problem is that differentiating numerically the data from Lai *et al.*, using central differences for example, brings some computation error. For this reason, in this work, is going to used the model proposed by Ribera and Myers [12] to compute $\bar{L}_m'^{\text{eff}}(R)$.
Replacing $\bar{L}_m^{\text{eff}}(R) = L_m^{RM}(R)$ (2.3) into the latent heat correction (equation (2.9)), it is obtained

$$L_m^{\text{eff}} = L_m^{\star} \left(1 - \left(1 - \frac{C}{3} \frac{R}{R_C} \right) e^{-C \frac{R}{R_C}} \right). \tag{2.10}$$

Then, the effective latent heat that is going to be used in this work, instead of following Figure 2.2, is going to be

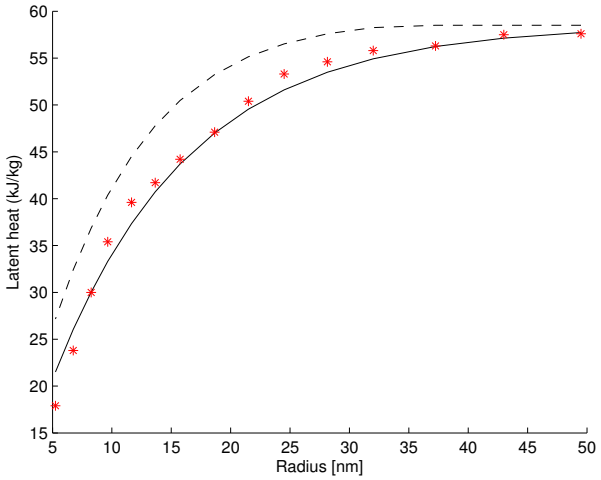

Figure 2.4: Correction of the latent heat data from Lai *et al.* [10]. The red asterisks are taken from Lai *et al.* [10]. The solid line corresponds to the exponential fitting (2.3) and the dashed line to its correction (2.10).

Summarizing, the measurements of effective latent heat done by Lai *et al.* [10] do not correspond to the definition of effective latent heat, this is the reason why it must be corrected. But as a spatial derivative must be computed, the exponential model proposed by Ribera and Myers [12] is going to be used to avoid computational error.

2.4 Results

In this Section, the models (2.2), (2.3) and (2.10) are going to be compared. The first model (2.2) comes from the melting depression of the melting temperature that is widely used, the problem of this model is that for tin $c_s \simeq c_l$ so the depression at the nanoscale will not be significant. The experiments from Lai *et al.* showed that the variation of latent heat is considerable, in consequence, Ribera and Myers proposed an exponential model (2.10) that fits really well the data from [10]. The problem is that these measures does not correspond to the definition of effective latent heat, for this reason, in this work is proposed a correction of the data from Lai *et al.* obtaining a corrected model (2.10). By construction, at the mascroscale all these models are going to bring the bulk value, but is at the nanoscale where these models disagree.

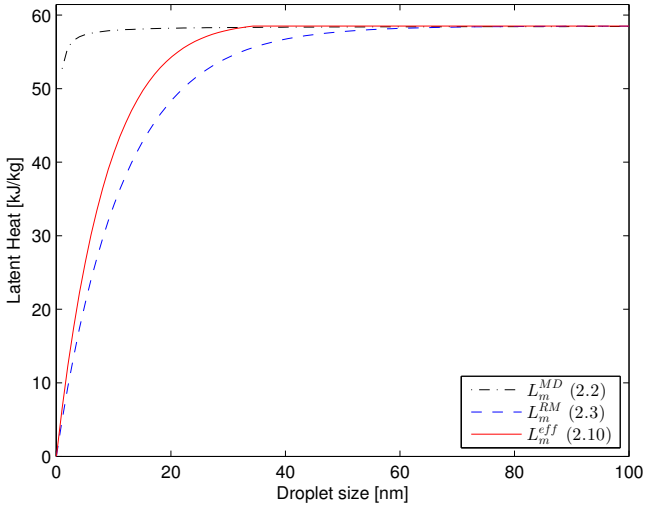

Figure 2.5: Size dependence of latent heat. The dashed dotted line in black corresponds to the effective latent heat of (2.2), the dashed line in blue to the equation (2.3) and the solid line in red to (2.10).

It is observed that for a radius higher than 50 nm the three models are close to the bulk value. Then a nanoparticle really bigger than 50 nm of diameter will melt according to the classical formulation. But is at the nanoscale where the three models differ. The model proposed by Ribera and Myers (2.3) is the first that decreases with radius and it reaches a half of the bulk value when the nanoparticle has 10 nm of radius, more or less. The model (2.10) begins to decrease a little bit later at 30 nm, while the effective latent heat proposed by (2.2) starts to decrease when the nanoparticle is almost molten. The fact of having $c_s \simeq c_l$, in the case of tin, makes the model (2.2) not far from considering a constant bulk value for the effective latent heat. It can be observed better the differences between models in Figure 2.6, where a zoom has been applied to Figure 2.5 cutting the x-axis at 10 nm.

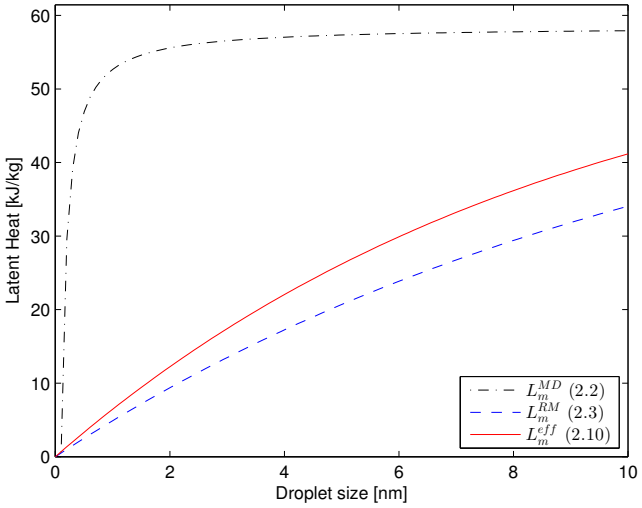

Figure 2.6: Size dependence of latent heat. The dashed dotted line in black corresponds to the effective latent heat of (2.2), the dashed line in blue to the equation (2.3) and the solid line in red to (2.10).

In this second situation, it is observed that the models (2.3) and (2.10) are far from the bulk value. For a radius of 10 nm, the effective latent heat is a 70% of $L_m^\star$ if the model (2.10) is used. In the case of (2.3), the effective latent heat is a 60% of $L_m^\star$.
Clearly, considering the expression (2.2) for latent heat implies an almost constant effective latent heat that only changes when the nanoparticle is almost molten. The Ribera and Myers model (2.3) and the correction (2.10) are more accurate because take into account the dependency of the effective latent heat with size. But in the previous section, it has been shown that (2.3) does not correspond to the definition of effective latent heat. Then, taking the model (2.3) is not accurate, because it will always bring lower melting times. This will be shown later, but first the reduction of the solid and the liquid problems must be introduced to obtain the ODE that drives the movement of the interface boundary.

Chapter 3

One phase reduction

3.1 Stefan problem

Once a size dependent expression for the effective latent heat is chosen, the Stefan condition introduced in the introduction (1.6) becomes

$$\rho_s L_m^{\text{eff}}(t) s_t = k_s \nabla\theta \cdot \mathbf{n}\Big|_{x=s} - k_l \nabla T \cdot \mathbf{n}\Big|_{x=s}. \tag{3.1}$$

To get an expression for the position of the interface, first of all, the liquid and the solid problems must be solved. In this Chapter, the solid problems is going to be simplified to get the one-phase reduction of the Stefan problem. This will reduce the problem to have only the liquid phase as unknown.
The solid and the liquid problems follow the heat equation (1.2) where heat is transmitted by diffusion, because in this work the liquid is treated as a solid $\mathbf{v} = 0$. Despite having a pressure jump at the interface due to the curvature of the surface, the liquid and the solid can be considered at constant pressure because $\mathbf{v} = 0$. Then $dp/dt = 0$ and using the chain rule, the first term of equation (1.2) is

$$\rho \frac{\partial h}{\partial t} = \rho \frac{dh}{dT}\Big|_p \frac{\partial T}{\partial t}. \tag{3.2}$$

Using the definition of specific heat at constant pressure $c_p = dh/dT$, the heat equation in each phase is

$$\rho c_p \frac{\partial T}{\partial t} - \nabla \cdot (k \nabla T) = 0, \tag{3.3}$$

using Fourier's law. The thermal conductivity k is treated as a constant. Then it is obtained the Laplace operator $\Delta = \nabla^2$ but, due to the geometry of the problem (see Figure 3.1), it must be expressed in spherical coordinates. If R is the position of the interface and R_0 the initial position of the interface the Stefan problem is

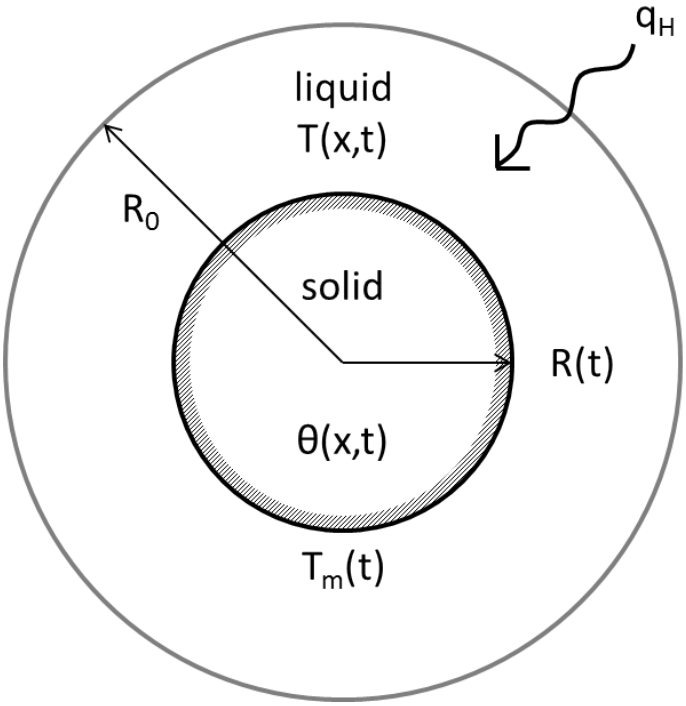

Figure 3.1: Geometry of the problem.

$$\rho_s c_s \frac{\partial \theta}{\partial t} = k_s \frac{1}{r^2} \frac{\partial}{\partial r}\left(r^2 \frac{\partial \theta}{\partial r}\right) \qquad \text{for } 0 < r < R(t), \tag{3.4a}$$

$$\rho_l c_l \frac{\partial T}{\partial t} = k_l \frac{1}{r^2} \frac{\partial}{\partial r}\left(r^2 \frac{\partial T}{\partial r}\right) \qquad \text{for } R(t) < r < R_0, \tag{3.4b}$$

$$\rho_s L_m^\star \left(1 - \left(1 - \frac{C}{3}\frac{R}{R_C}\right) e^{-C\frac{R}{R_C}}\right) R_t = k_s \left.\frac{d\theta}{dr}\right|_{r=R} - k_l \left.\frac{dT}{dr}\right|_{r=R}. \tag{3.4c}$$

As said in the Introduction, the difference of this work with other papers are the variation of the latent heat and the boundary condition used for the liquid problem. Instead of a Dirichlet condition, a Newton cooling condition is going to be used at $r = R_0$. Due to the geometry of the problem, at $r = 0$ there is a symmetry boundary condition. At the melting interface, to couple the solid and the liquid problems, the continuity of temperature will be ensured using the melting temperature and the heat flux will be conserved using the Stefan condition (3.4c). Adding the initial condition, the boundary conditions are

$$\begin{aligned} \left.\frac{\partial \theta}{\partial t}\right|_{r=0} &= 0, & \theta(R,t) = T(R,t) &= T_m(t), \\ -k_l \left.\frac{\partial T}{\partial r}\right|_{r=R_0} &= \alpha\left(T(R,t) - T_H\right), & \theta(r,0) &= T_m(0), \end{aligned} \tag{3.5}$$

Initially, for simplicity, it is considered that the solid is at the melting temperature and it is ready to melt.

3.2 Dimensionless formulation

To simplify the problem is going to be used the dimensionless problem. The dimensionless variables that are going to be used are the following

$$\hat{T} = \frac{T - T_m^\star}{T_H - T_m^\star}, \quad \hat{\theta} = \frac{\theta - T_m^\star}{T_H - T_m^\star}, \quad \hat{T}_m = \frac{T_m - T_m^\star}{T_H - T_m^\star}, \quad \hat{L}_m = \frac{L_m}{L_m^\star}, \\ \hat{r} = \frac{r}{R_0}, \quad \hat{R} = \frac{R}{R_0}, \quad \hat{t} = \frac{k_l}{\rho_s c_l R_0^2} t. \tag{3.6}$$

The length-scale R_0 is the initial size of the nanoparticle and the temperature-scale has been chosen to get 0 temperature at the bulk melting temperature and 1 at the surrounding temperature. The time-scale has been chosen simply to reduce the heat equations as Myers and Font did in [11]. In this work are going to be used the following dimensionless parameters

$$k = \frac{k_s}{k_l}, \qquad c = \frac{c_s}{c_l}, \qquad \Gamma = \frac{\sigma_{sl}^\star T_m^\star}{R_0 \rho_s L_m^\star (T_H - T_m^\star)}, \\ \lambda = \frac{C}{3}\frac{R_0}{R_C}, \qquad \mathrm{Nu} = \frac{\alpha R_0}{k_l}, \qquad \beta = \frac{L_m^\star}{c_l (T_H - T_m^\star)}. \tag{3.7}$$

The parameter Γ has been taken from Font and Myers [8] and it is used for the dimensionless version of the melting temperature (2.1) and it will also appear in the melting depression expression for the effective latent heat (2.2). This parameter looks similar to the capillary constant introduced in Alexiades and Solomon [2] that in this work is R_C. The Nusselt number compares the heat transmitted by conduction in the nanoparticle with the heat convected with the surroundings using the Newton cooling condition. Finally β is the inverse of the Stefan number that compares the latent heat with the sensible heat in the liquid. The latent heat is the heat related to the change of mass while the sensible heat is related to the change of temperature. Then the problem becomes, dropping off the hats,

$$\frac{\partial \theta}{\partial t} = \frac{k}{c}\frac{1}{r^2}\frac{\partial}{\partial r}\left(r^2 \frac{\partial \theta}{\partial r}\right) \qquad \text{for } 0 < r < R(t), \tag{3.8a}$$

$$\frac{\partial T}{\partial t} = \frac{1}{r^2}\frac{\partial}{\partial r}\left(r^2 \frac{\partial T}{\partial r}\right) \qquad \text{for } R(t) < r < 1, \tag{3.8b}$$

$$\beta\left(1 - (1 - \lambda R)\, e^{-3\lambda R}\right) R_t = k \left.\frac{\partial \theta}{\partial r}\right|_{r=R(t)} - \left.\frac{\partial T}{\partial r}\right|_{r=R(t)}, \tag{3.8c}$$

with boundary conditions

$$\left.\frac{\partial \theta}{\partial t}\right|_{r=0} = 0, \qquad \theta(R,t) = T(R,t) = -2\frac{\Gamma}{R}, \\ -\left.\frac{\partial T}{\partial r}\right|_{r=1} = \mathrm{Nu}\,(T(1,t) - 1), \qquad \theta(R,0) = T(R,0) = -2\Gamma. \tag{3.9}$$

The three expressions for effective latent heat (2.2), (2.3) and (2.9) become, respectively

$$L_m^{MD} = 1 - 2\frac{1-c}{\beta}\frac{\Gamma}{R}, \tag{3.10a}$$

$$L_m^{RM} = 1 - e^{-3\lambda R}, \tag{3.10b}$$

$$L_m^{\text{eff}} = 1 - (1-\lambda R)\, e^{-3\lambda R}. \tag{3.10c}$$

The differences of three models is how they decrease with radius. The first dimensionless latent heat expression (3.10a) tends to $-\infty$ when $R \to 0$. Physically it has no sense because a negative latent heat means that the nanoparticle instead of melting is solidifying and an infinite latent heat means that it needs infinite energy to change phase, but there is no mass to melt when $R = 0$. Another problem is that, working with tin implies $c \simeq 1$ and $\beta \gg 1$. Then $(1-c)/\beta \ll 1$ so the decrease of latent heat is not significant and it only appears when the nanoparticle has almost melted, as shown before in Section 2.4. About the other two models for effective latent heat (3.10b) and (3.10c), they differ in the coefficient of the exponential. When $R \ll 1$, using infinitesimal equivalences

$$L_m^{RM} \sim 1 - (1 - 3\lambda R) = 3\lambda R, \tag{3.11a}$$

$$L_m^{\text{eff}} \sim 1 - (1-\lambda R)\,(1-3\lambda R) = 4\lambda R + 3\lambda^2 R^2 \sim 4\lambda R. \tag{3.11b}$$

Both models have more sense than (3.10a) because they tend to 0 when $R \to 0$. The difference between (3.10b) and (3.10c) is that $L_m^{RM} < L_m^{\text{eff}}$, then the L_m^{RM} will always give faster melting. Now, once the Stefan problem has been non-dimensionalized, it is time to reduce the problem into an ODE.

3.3 Large conductivity reduction

The first reduction comes from considering that the conductivity in the solid is really large compared to the liquid part $k_s > k_l$. Then the conductivity dimensionless parameter $k = k_s/k_l \gg 1$ is really large and the solid problem (3.8a) can be approximated to a Laplace's equation

$$\frac{1}{k}\frac{\partial\theta}{\partial t} = \frac{1}{c}\frac{1}{r^2}\frac{\partial}{\partial r}\left(r^2\frac{\partial\theta}{\partial r}\right) \simeq 0 \text{ with } \frac{\partial\theta}{\partial r}(0) = 0 \text{ and } \theta(R) = -2\frac{\Gamma}{R}. \tag{3.12}$$

As the symmetry leaves free the boundary at $r = 0$ the solid temperature will be completely driven by the melting temperature. This means that the temperature in the solid will be $\theta(r,t) \simeq -2\Gamma/R(t)$. This approximation is known as one-phase reduction and it corresponds to the leading order of the perturbed solution for the solid. As said in the Introduction, a perturbed solution is an approximation of the solution using a power series of a small parameter. In the case of the solid problem, the small parameter corresponds to $1/k$.

$$\theta(r,t) = \theta_0(r,t) + \frac{1}{k}\theta_1(r,t) + \frac{1}{k^2}\theta_2(r,t) + \mathcal{O}\left(\frac{1}{k^3}\right). \tag{3.13}$$

Replacing this perturbed solution (3.13) into equation (3.8a) the solid problem becomes

$$\frac{1}{k}\theta_{0t} + \frac{1}{k^2}\theta_{1t} + \mathcal{O}\left(\frac{1}{k^2}\right) = \frac{1}{c}\left[\frac{2}{r}\theta_{0r} + \theta_{0rr}\right] + \frac{1}{k}\frac{1}{c}\left[\frac{2}{r}\theta_{1r} + \theta_{1rr}\right] + \mathcal{O}\left(\frac{1}{k^2}\right), \tag{3.14}$$

where the boundary conditions are

$$\theta(R,t) = -2\frac{\Gamma}{R} \Rightarrow \begin{cases} \theta_0(R,t) = -2\frac{\Gamma}{R} \\ \theta_i(R,t) = 0 \qquad i > 0 \end{cases}, \tag{3.15a}$$

$$\theta_r(0,t) = 0 \Rightarrow \theta_{ir}(0,t) = 0 \ \ \forall i. \tag{3.15b}$$

Grouping terms with the same power of $1/k$, the following differential equations are obtained

$$\mathcal{O}(1): \qquad 0 = \frac{2}{r}\theta_{0r} + \theta_{0rr}, \quad \theta_{0r}(0,t) = 0, \quad \theta_0(R,t) = -2\frac{\Gamma}{R}. \tag{3.16a}$$

$$\mathcal{O}\left(\frac{1}{k}\right): \quad c\,\theta_{0t} = \frac{2}{r}\theta_{1r} + \theta_{1rr}, \quad \theta_{1r}(0,t) = 0, \qquad \theta_1(R,t) = 0. \tag{3.16b}$$

Where the zero order term (3.16a) corresponds to an ODE in space whose solution is of the form

$$\theta_{0r} = \frac{C_1(t)}{r^2}. \tag{3.17}$$

Using the boundary condition at $r = 0$ from (3.16a) the coefficient is $C_1(t) = 0$. It means that θ_0 is constant in space. Finally, using the boundary condition at $r = R$ from (3.16a) the leading order of the perturbed solution will be

$$\theta_0(r,t) = -2\frac{\Gamma}{R(t)}, \tag{3.18}$$

as stated before at the beginning of this section. Taking the zero order solution (3.18), the first order differential equation (3.16b) becomes an ODE

$$2\frac{c\,\Gamma}{R^2}R_t = \frac{2}{r}\theta_{1r} + \theta_{1rr}, \qquad \theta_{1r}(0,t) = 0, \qquad \theta_1(R,t) = 0. \tag{3.19}$$

To solve this ODE (3.19) a new function is defined $v := \theta_{1r}$ to solve easier the ODE. First, the homogeneous ODE is solved which solution has been computed before, $v^h = C_1(t)/r^2$. Then the particular solution is of the form $v^p = u(r,t)/r^2$. Introducing it into the ODE (3.19)

$$\frac{2}{r}v_p + v_{pr} = \frac{2}{\cancel{r}}\frac{\cancel{u(r)}}{r^2} + \frac{u'(r)}{r^2} - 2\frac{\cancel{u(r)}}{r^3} = 2\frac{c\,\Gamma}{R^2}R_t \Rightarrow u(r,t) = \frac{2}{3}\frac{c\,\Gamma}{R^2}R_t r^3. \tag{3.20}$$

Then the solution for v will be of the form

$$v = v^h + v^p = \frac{C_1(t)}{r^2} + \frac{2}{3}\frac{c\,\Gamma}{R^2}R_t r, \tag{3.21}$$

that using the symmetry boundary condition in (3.19) the coefficient $C_1(t) = 0$. Then as $v = \theta_{1r}$, integrating, it is obtained the perturbed solution corresponding the first power of $1/k$

$$\theta_1(r,t) = \frac{1}{3}\frac{c\,\Gamma}{R^2} R_t r^2 + C_2(t). \tag{3.22}$$

Finally, imposing the boundary condition at the interface from (3.19), the first order solution for the solid is

$$\theta_1(r,t) = \frac{c\,\Gamma}{3}\frac{r^2 - R^2}{R^2} R_t. \tag{3.23}$$

Then the perturbation solution for the temperature of the solid problem in terms of small parameter $1/k$ to first order is

$$\theta(r,t) = -2\frac{\Gamma}{R} + \frac{c\,\Gamma}{k\,3}\frac{r^2 - R^2}{R^2} R_t + \mathcal{O}\left(k^{-2}\right), \tag{3.24}$$

where the temperature of the solid is not constant anymore in space, as is usually supposed taking the leading order of (3.24). The term associated to the first order perturbed solution is positive because the nanoparticle is shrinking and $R_t < 0$. Then surprisingly, at the nanoscale, the solid temperature is higher than the interface temperature.
This liquid temperature profile will contribute to the Stefan condition with a heat flux different from zero, so using the first order perturbed solution is more accurate [11]. The solid term of the Stefan condition will be

$$\frac{\partial \theta}{\partial r}(R,t) = \frac{2}{3}\frac{c}{k}\frac{\Gamma}{R} R_t + \mathcal{O}(k^{-2}). \tag{3.25}$$

Finally replacing (3.25) to the new Stefan boundary condition (3.8c)

$$\left[\beta\left(1 - (1 - \lambda R)\, e^{-3\lambda R}\right) - \frac{2}{3}\frac{c}{k}\frac{\Gamma}{R}\right] R_t = -\left.\frac{\partial T}{\partial r}\right|_{r=R(t)}, \tag{3.26}$$

correct to $\mathcal{O}(k^{-1})$. As said before, the Stefan condition (3.26) corresponds to the one-phase reduction because the solid part is not a problem anymore. Now there is still the liquid as unknown of the Stefan problem.

Chapter 4

Effect of the outer boundary condition

In this Chapter, the liquid temperature profile is going to be approximated using a perturbed solution to reduce the Stefan problem into a first order ODE. The most famous boundary conditions applied to the liquid problem are the Dirichlet and the Newton cooling boundary conditions. The first one is usually chosen for mathematical convenience because it simplifies the computations. Otherwise, it implies an infinite heat transfer, for this reason the second one has more sense physically.
In this work, for the reduction of the liquid problem, the Robin condition is going to be used. To compare it with the other boundary condition, the Dirichlet boundary condition can be recovered taking $\mathrm{Nu} \to \infty$ using the same formulation.

4.1 Large β reduction

The reduction of the liquid problem will come from considering $\beta \gg 1$ (for gold heated 10°C above the bulk melting temperature $\beta \simeq 40$ [8]). This means that, using the definition of β that was introduced in (3.7), the latent heat dominates the sensible heat. In other words, the energy related to the change of temperature is insignificant compared to the energy related to the change of mass. The heat transfer equations are quasi-static compared to the dynamics of the interface boundary. Then, as done in Section 3.3, the liquid problem can be approximated to a Laplace's equation

$$\frac{\partial T}{\partial t} = \frac{1}{r^2}\frac{\partial}{\partial r}\left(r^2 \frac{\partial T}{\partial r}\right) \simeq 0 \text{ with } T(R) = -2\frac{\Gamma}{R} \text{ and } -\frac{\partial T}{\partial r}(1) = \mathrm{Nu}\,(T(1) - 1)). \tag{4.1}$$

In this case, for the liquid problem, the perturbed solution approximation takes $1/\beta$ as small parameter

$$T(r,t) = T_0(r,t) + \frac{1}{\beta}T_1(r,t) + \frac{1}{\beta^2}T_2(r,t) + \mathcal{O}\left(\frac{1}{\beta^3}\right). \tag{4.2}$$

Replacing the perturbed solution (4.2) into the liquid equation (3.8b) and re-scaling in time using $t = \beta\tau$, it is obtained

$$\frac{1}{\beta}T_{0\tau}+\frac{1}{\beta^2}T_{1\tau}+\mathcal{O}\left(\frac{1}{\beta^2}\right) = \left[\frac{2}{r}T_{0r} + T_{0rr}\right]+\frac{1}{\beta}\left[\frac{2}{r}T_{1r} + T_{1rr}\right]+\mathcal{O}\left(\frac{1}{\beta^2}\right), \quad (4.3)$$

because $\partial_t = \frac{1}{\beta}\partial_\tau$. Where the boundary conditions now are

$$\begin{aligned} T(R,\tau) = -2\frac{\Gamma}{R} \Rightarrow \begin{cases} T_0(R,\tau) = -2\frac{\Gamma}{R} \\ T_i(R,\tau) = 0 \qquad i>0 \end{cases}, \\ T_r(1,\tau) = \mathrm{Nu}\,(1-T(1,\tau)) \Rightarrow \begin{cases} T_{0r}(1,\tau) = \mathrm{Nu}\,(1-T_0(1,\tau)) \\ T_{ir}(1,\tau) = -\mathrm{Nu}\;T_i(1,\tau) \qquad i>0 \end{cases}. \end{aligned} \quad (4.4)$$

Grouping terms with the same power of $1/\beta$, for the liquid problem, the differential equations to solve are

$$\mathcal{O}(1): \qquad 0 = \frac{2}{r}T_{0r} + T_{0rr}, \quad T_0(R) = -2\frac{\Gamma}{R}, \quad T_{0r}(1) = \mathrm{Nu}\,(1-T_0(1))\,. \quad (4.5a)$$

$$\mathcal{O}\left(\frac{1}{\beta}\right): \quad T_{0\tau} = \frac{2}{r}T_{1r} + T_{1rr}, \qquad T_1(R) = 0, \qquad T_{1r}(1) = -\mathrm{Nu}\;T_1(1). \quad (4.5b)$$

As before, the zero order term (4.5a) corresponds to an ODE in space whose solution is of the form

$$\frac{2}{r}T_{0r} + T_{0rr} = 0, \quad T_0(R) = -2\frac{\Gamma}{R}, \quad T_{0r}(1) = \mathrm{Nu}\,(1-T_0(1,\tau))\,. \quad (4.6)$$

Which solution, in general form, will be

$$T_0(r,\tau) = -\frac{C_1(\tau)}{r} + C_2(\tau) \quad (4.7)$$

where $C_1(\tau)$ and $C_2(\tau)$ are constants in space. Then imposing the boundary conditions (4.4)

$$-\frac{C_1(\tau)}{R} + C_2(\tau) = -2\frac{\Gamma}{R}, \quad (4.8a)$$

$$C_1(\tau) = \mathrm{Nu}\,(1 + C_1(\tau) - C_2(\tau))\,, \quad (4.8b)$$

are obtained the following coefficients

$$C_1(\tau) = \frac{R\,\mathrm{Nu}\left(1+2\frac{\Gamma}{R}\right)}{R+\mathrm{Nu}\,(1-R)}, \quad (4.9a)$$

$$C_2(\tau) = -2\frac{\Gamma}{R} + \frac{\mathrm{Nu}\left(1+2\frac{\Gamma}{R}\right)}{R+\mathrm{Nu}\,(1-R)}. \quad (4.9b)$$

That replacing them in (4.7), the zero order perturbed solution for the liquid is

$$T_0(r,\tau) = -2\frac{\Gamma}{R} + \frac{\mathrm{Nu}\,(R+2\Gamma)}{R+\mathrm{Nu}\,(1-R)}\left(\frac{1}{R}-\frac{1}{r}\right), \tag{4.10}$$

where $R = R(\tau)$. To simplify the next steps, the leading order solution can be rewritten as

$$T_0(r,\tau) = F_1(\tau) + \frac{F_2(\tau)}{r}, \tag{4.11}$$

where

$$F_1(\tau) = -2\frac{\Gamma}{R} - \frac{F_2(\tau)}{R}, \tag{4.12a}$$

$$F_2(\tau) = -\frac{\mathrm{Nu}\,(R+2\Gamma)}{R+\mathrm{Nu}\,(1-R)}. \tag{4.12b}$$

Then, the differential equation corresponding to the first power of $1/\beta$ (4.5b) becomes an ODE

$$2\frac{2}{r}T_{1r} + T_{1rr} = \frac{\partial F_1}{\partial\tau} + \frac{1}{r}\frac{\partial F_2}{\partial\tau}, \quad T_1(R) = 0, \quad T_{1r}(1) = -\mathrm{Nu}\;T_1(1,\tau). \tag{4.13}$$

As before with the solid solution, it is defined a new function $w := T_{1r}$ to solve the liquid ODE (4.13). Where the homogeneous solution is $w^h = C_1(\tau)/r^2$. Then the particular solution should be $w^p = u(r,\tau)/r^2$. That replacing it in the ODE (4.13)

$$\frac{2}{r}w_p + w_{pr} = \frac{u'(r)}{r^2} - = \frac{\partial F_1}{\partial\tau} + \frac{1}{r}\frac{\partial F_2}{\partial\tau} \Rightarrow u(r,\tau) = \frac{\partial F_1}{\partial\tau}\frac{r^3}{3} + \frac{\partial F_2}{\partial\tau}\frac{r^2}{2}. \tag{4.14}$$

Then the general solution of $w = T_{1r}$ will be

$$w = \frac{C_1(\tau)}{r^2} + \frac{1}{3}\frac{\partial F_1}{\partial\tau}\,r + \frac{1}{2}\frac{\partial F_2}{\partial\tau}, \tag{4.15}$$

that integrating in space it is obtained a general expression for T_1

$$T_1(r,\tau) = -\frac{C_1(\tau)}{r} + \frac{1}{6}\frac{\partial F_1}{\partial\tau}r^2 + \frac{1}{2}\frac{\partial F_2}{\partial\tau}\,r + C_2(\tau), \tag{4.16}$$

where $C_1(\tau)$ and $C_2(\tau)$ are constants in space. Now imposing the boundary conditions in (4.13)

$$-\frac{C_1(\tau)}{R} + \frac{1}{6}\frac{\partial F_1}{\partial\tau}R^2 + \frac{1}{2}\frac{\partial F_2}{\partial\tau}R + C_2(\tau) = 0, \tag{4.17a}$$

$$C_1(\tau) + \frac{1}{3}\frac{\partial F_1}{\partial\tau} + \frac{1}{2}\frac{\partial F_2}{\partial\tau} = -\mathrm{Nu}\left(-C_1(\tau) + \frac{1}{6}\frac{\partial F_1}{\partial\tau} + \frac{1}{2}\frac{\partial F_2}{\partial\tau} + C_2(\tau)\right), \tag{4.17b}$$

the coefficients are

$$C_1(\tau) = R\frac{\frac{1}{3}\frac{\partial F_1}{\partial\tau}\left(\frac{\mathrm{Nu}}{2}\left(R^2-1\right)-1\right) + \frac{1}{2}\frac{\partial F_2}{\partial\tau}\left(\mathrm{Nu}\,(R-1)-1\right)}{R+\mathrm{Nu}\,(1-R)}, \tag{4.18a}$$

$$C_2(\tau) = \frac{C_1(\tau)}{R} - \frac{1}{6}\frac{\partial F_1}{\partial \tau}R^2 - \frac{1}{2}\frac{\partial F_2}{\partial \tau}R, \tag{4.18b}$$

Replacing these constants in (4.16) it is obtained

$$T_1(r,\tau) = F_3(\tau)\left(\frac{1}{R} - \frac{1}{r}\right) + \frac{1}{6}\frac{\partial F_1}{\partial \tau}\left(r^2 - R^2\right) + \frac{1}{2}\frac{\partial F_2}{\partial \tau}\left(r - R\right), \tag{4.19}$$

where $F_3(\tau) = C_1(\tau)$. Then the perturbed solution of the liquid to first order is

$$T(r,\tau) = F_1(\tau) + \frac{F_2(\tau)}{r} + \frac{r-R}{\beta}\left(\frac{F_3(\tau)}{R\,r} + \frac{1}{6}\frac{\partial F_1}{\partial \tau}\left(r + R\right) + \frac{1}{2}\frac{\partial F_2}{\partial \tau}\right) + \mathcal{O}(\beta^{-2}). \tag{4.20}$$

The liquid contribution into the Stefan condition is

$$\frac{\partial T}{\partial r}(r,\tau) = \left(\frac{F_3(\tau)}{\beta} - F_2(\tau)\right)\frac{1}{r^2} + \frac{1}{\beta}\left(\frac{1}{3}\frac{\partial F_1}{\partial \tau}r + \frac{1}{2}\frac{\partial F_2}{\partial \tau}\right) + \mathcal{O}(\beta^{-2}), \tag{4.21}$$

but first, the original time is recovered using $\partial_t = \frac{1}{\beta}\partial_\tau$

$$\frac{\partial T}{\partial r}(r,t) = \left(F_3(t) - F_2(t)\right)\frac{1}{r^2} + \frac{1}{3}\frac{\partial F_1}{\partial t}r + \frac{1}{2}\frac{\partial F_2}{\partial t} + \mathcal{O}(\beta^{-2}), \tag{4.22}$$

where

$$F_2(t) = -\frac{\mathrm{Nu}\left(R + 2\Gamma\right)}{R + \mathrm{Nu}\left(1 - R\right)}, \tag{4.23a}$$

$$\frac{\partial F_2(t)}{\partial t} = -\mathrm{Nu}\frac{\mathrm{Nu} + 2\Gamma\left(\mathrm{Nu} - 1\right)}{\left(R + \mathrm{Nu}\left(1 - R\right)\right)^2}R_t, \tag{4.23b}$$

$$\frac{\partial F_1}{\partial t}(t) = \frac{2\Gamma + F_2}{R^2}R_t - \frac{1}{R}\frac{\partial F_2}{\partial t}, \tag{4.23c}$$

$$F_3(t) = R\frac{\frac{1}{3}\frac{\partial F_1}{\partial t}\left(\frac{\mathrm{Nu}}{2}\left(R^2 - 1\right) - 1\right) + \frac{1}{2}\frac{\partial F_2}{\partial t}\left(\mathrm{Nu}\left(R - 1\right) - 1\right)}{R + \mathrm{Nu}\left(1 - R\right)}. \tag{4.23d}$$

To simplify the formulation, the following variables are going to be used

$$f_2(t) = -\mathrm{Nu}\frac{\mathrm{Nu} + 2\Gamma\left(\mathrm{Nu} - 1\right)}{\left(R + \mathrm{Nu}\left(1 - R\right)\right)^2} \Rightarrow \frac{\partial F_2}{\partial t} = f_2(t)R_t, \tag{4.24a}$$

$$f_1(t) = \frac{2\Gamma + F_2}{R^2} - \frac{1}{R}f_2(t) \Rightarrow \frac{\partial F_1}{\partial t} = f_1(t)R_t, \tag{4.24b}$$

$$f_3(t) = R\frac{\frac{f_1(t)}{3}\left(\frac{\mathrm{Nu}}{2}\left(R^2 - 1\right) - 1\right) + \frac{f_2(t)}{2}\left(\mathrm{Nu}\left(R - 1\right) - 1\right)}{R + \mathrm{Nu}\left(1 - R\right)} \Rightarrow F_3 = f_3(t)R_t, \tag{4.24c}$$

reducing the expression of the liquid's contribution to the Stefan condition

$$\frac{\partial T}{\partial r}(R,t) = \left(\frac{1}{3}f_1(t)R + \frac{1}{2}f_2(t) + \frac{f_3(t)}{R^2}\right)R_t - \frac{F_2(t)}{R^2} + \mathcal{O}(\beta^{-2}). \tag{4.25}$$

Now the contribution of the liquid to the Stefan condition (4.25) can be replaced into the one-phase problem (3.26)

$$\left[\beta\left(1-(1-\lambda R)\,e^{-3\lambda R}\right)-f_\theta(t)+\frac{1}{3}f_1(t)R+\frac{1}{2}f_2(t)+\frac{f_3(t)}{R^2}\right]R_t=\frac{F_2(t)}{R^2}, \tag{4.26}$$

correct to $\mathcal{O}(k^{-1}+\beta^{-1})$. Where $f_\theta(t)=\frac{2}{3}\frac{c}{k}\frac{\Gamma}{R}$. The right hand side term of (4.26) corresponds to the leading order of the perturbed solution and the first order term is introduced in the Stefan condition as a coefficient of R_t.
This second reduction (4.26) is known as the two-phase formulation [7]. This large β reduction, could have been used in the solid problem re-scaling the time, but the final perturbed solution is independent of the small parameter ε chosen, when the original time is recovered. Despite this, physically is commonly used the large conductivity simplification for the solid problem, especially with metals. Now, with this two-phase formulation, the unique unknown of the Stefan problem is the position of the interface that is obtained solving the ODE in (4.26).

4.2 Nusselt number

The previous reduction of the Stefan problem depends on the Nu number. The Nu number indicates how heat is convected with the surroundings in the boundary of the domain. To approximate a value for Nu without solving the whole liquid problem, it has been considered the steady state problem with the surrounding temperature at infinity. Then, after solving the heat problem, is going be searched the Nu number corresponding to this problem.
The solution for the Laplace's equation in spherical coordinates has been obtained before

$$T(r)=-\frac{C_1}{r}+C_2, \tag{4.27}$$

but, taking into account that the surrounding is placed at infinity, now the boundary conditions are

$$\lim_{r\to\infty}=C_2=1, \tag{4.28a}$$

$$T(R)=-\frac{C_1}{R}+C_2=-2\frac{\Gamma}{R}. \tag{4.28b}$$

Then $C_1=2\Gamma+R$. So the solution of the liquid heat equation is

$$T(r)=-\frac{2\Gamma+R}{r}+1, \tag{4.29}$$

where the temperature at the boundary of the domain is $T(1)=1-2\Gamma-R$ and the heat flux is $-T'(1)=-2\Gamma-R$. Then using the Newton cooling condition

$$-T'(1)=\mathrm{Nu}(T(1)-1), \tag{4.30}$$

this means that the Nusselt number must be of the order $\mathrm{Nu}=\mathcal{O}(1)$. In Ribera and Myers [12] is chosen the highest value for the heat transfer coefficient α

which still permits thermodynamic stability, but in this work, for simplicity, it will be considered Nu=1.
The choice of Nu only affects the liquid problem. The leading order of the perturbed solution (4.10) becomes

$$T_0(r,\tau) = -2\frac{\Gamma}{r} + 1 - \frac{R}{r}, \tag{4.31}$$

where $T_0 \simeq -2\frac{\Gamma}{r}$, the Gibbs-Thomson relation (2.1), if $\Gamma \gg 1$. On the other hand, the first order term (4.19) becomes

$$\frac{1}{\beta}T_1(r,\tau) = \frac{r-R}{2}\left[\frac{2-R}{r} - 1\right] R_t, \tag{4.32}$$

where $r - R > 0$ because at the liquid $r > R$, $2 - R - r > 0$ because $r < 1$ and $R < 1$ then $r + R < 2$ and, finally, $R_t < 0$ because the nanoparticle is melting. This means that the contribution of the first order term is always negative and will give colder solutions than the temperature delivered by the leading order term. It should been also noted, as stated in the previous Section, that recovering the initial time from τ makes the perturbed solution independent of the perturbed parameter β. This change of the liquid profile also affect the liquid contribution to the Stefan condition. Replacing Nu=1 into the previous variables (4.23a), (4.24a), (4.24b) and (4.24c)

$$F_2(t) = -R - 2\Gamma, \tag{4.33a}$$

$$f_2(t) = -1, \tag{4.33b}$$

$$f_1(t) = 0, \tag{4.33c}$$

$$f_3(t) = \frac{R}{2}(2-R), \tag{4.33d}$$

the Stefan condition (4.26) becomes

$$\left[\beta\left(1 - (1-\lambda R)\, e^{-3\lambda R}\right) - \frac{2}{3}\frac{c}{k}\frac{\Gamma}{R} - \frac{1}{2} + \frac{2-R}{2\,R}\right] R_t = \frac{F_2(t)}{R^2}. \tag{4.34}$$

If $\beta \gg 1$, the Stefan condition is not affected by the order of the perturbed solution, because the first term is dominant. But if it is not the case, the effective latent heat will change if the first order perturbed solution is used, according to

$$\beta\left(1 - (1-\lambda R)\, e^{-3\lambda R}\right) + \left(1 - \frac{2}{3}\frac{c\,\Gamma}{k}\right)\frac{1}{R} - 1. \tag{4.35}$$

Then if $k \gg 1$, there is a positive contribution to the effective latent heat that makes the first order solution slower than the zero order perturbed solution.

4.3 Dirichlet boundary condition

Using the same formulation for the two-phase reduction introduced in Section 4.1, the Dirichlet boundary condition can be recovered taking Nu$\to \infty$. The only parameters that depend on Nu, as said in the previous Section, are (4.23a), (4.24a) and (4.24c). Taking limits, these parameters become

$$F_2(t) = -\frac{R + 2\Gamma}{1 - R}, \tag{4.36a}$$

$$f_2(t) = -\frac{1 + 2\Gamma}{(1 - R)^2}, \tag{4.36b}$$

$$f_3(t) = -\frac{R}{2}\left(\frac{R+1}{3} f_1(t) + f_2(t)\right). \tag{4.36c}$$

Now the two boundary conditions for the liquid can be compared but first, a discussion of the order of the perturbed solution is going to be done.

4.4 Order of the perturbed solution

In this section are going to be compared the zero order and the first order solutions for the two-phase problem. As said in Section 4.1, the two-phase problem reduces the Stefan problem to an ODE for the position of the interface. The leading order of the perturbed solutions appears on the right hand side of the ODE (see equation (4.26)) while the first order term of the perturbed solution contributes as a coefficient of R_t.
To see the differences between taking the first order perturbed solution or simply taking the leading order as the solution, the parameters T_H and R_0 have been taken as parameters. The tin properties have been taken from Table 4.1.

Material	$T_m^\star$ [K]	$L_m^\star$ [J/kg]	c_s/c_l [J/kg K]	k_s/k_l [W/m K]	ρ_s [kg/m^3]	$\sigma_{sl}^\star$ [N/m]
Tin	505	58500	230/268	67/30	7180	0,064

Table 4.1: Tin properties, taken from Ribera and Myers [12].

For the initial radius is going to be considered $R_0 = 10$ nm and $R_0 = 100$ nm. For the surrounding temperature, has been considered $T_H = T_m^\star + 2,2$ and $T_H = T_m^\star + 22$ corresponding to $\beta = 100$ and $\beta = 10$, respectively. For the following plots, the dotted line in black corresponds to the interface temperature during melting according to (2.1). The other colours correspond to the liquid and the solid profiles for different positions of the moving boundary.

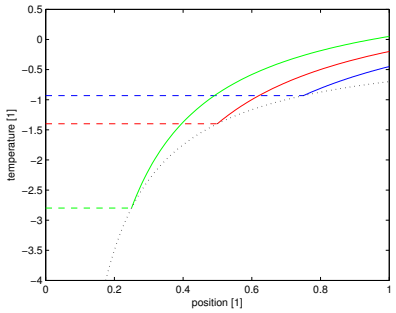

Figure 4.1: Leading order with $\beta = 10$ and $R_0 = 10$ nm.

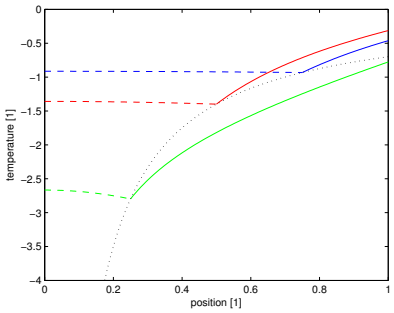

Figure 4.2: 1st order solution with $\beta = 10$ and $R_0 = 10$ nm.

In this first situation it can be observed that the solution is different when the nanoparticle is little (green). Close to the melting time, the solid distribution of temperature is not constant (green line of Figure 4.2). Then a heat flux from the solid appears in the Stefan condition that before was zero (blue and red lines of Figure 4.2). As stated before, the liquid temperature profile is colder for the first order perturbed solution. While in the zero order solution (see Figure 4.1) the liquid temperature in green is above the interface temperature curve, in the first order solution (see Figure 4.2) is beyond the dotted line.
Now changing the surrounding temperature to obtain $\beta = 100$.

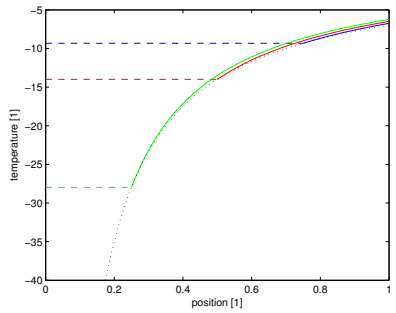

Figure 4.3: Leading order, $\beta = 100$ and $R_0 = 10$ nm.

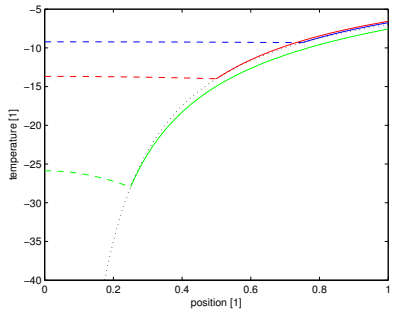

Figure 4.4: 1st order solution, $\beta = 100$ and $R_0 = 10$ nm.

In the leading order solution (see Figure 4.3) it is observed that the liquid follows (1.1), the black dotted line, because $\Gamma \gg 1$. In Figure 4.4 as before, when the particle is close to melting time, the solid profile is not constant. Also, a colder solution for the liquid profile is obtained, that is beyond the interface temperature (black dotted line).
Changing the initial radius to $R_0 = 100$ nm, with $\beta = 10$ the liquid reaches different temperatures at the boundary depending on the order of the perturbed solution, while the profile in the solid is constant always (see Figures 4.5 and (4.6)). At the beginning of the melting, the temperature of the liquid is colder if a first order perturbed solution is used instead of using the leading order.

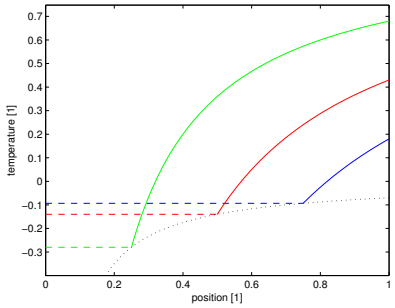

Figure 4.5: Leading order, $\beta = 10$ and $R_0 = 100$ nm.

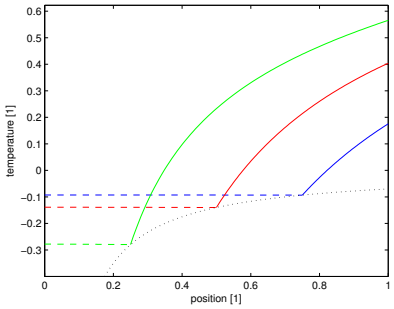

Figure 4.6: 1st order solution, $\beta = 10$ and $R_0 = 100$ nm.

Finally, for the combination $\beta = 100$ and $R_0 = 100$ nm there is no difference between using the leading order or the first order perturbed solution. Summarizing, taking a first order perturbed solution makes the solid profile non-constant in space at the nanoscale, contradicting the usual supposition taken in the one-phase reduction. This makes appear a heat flux at the interface that usually does not affect the Stefan condition. Another phenomenon that appears with the first order perturbed solution, is that the liquid is colder than taking only the leading order term. This increases the influx on the outer boundary because of the Newton cooling condition. These two phenomena make that taking the leading order is inaccurate for the liquid and the solid. In the next Section, the two outer boundary conditions will be compared.

4.5 Results

In this Section, the functions (4.33a), (4.33b) and (4.33d) are going to be used to apply the Robin boundary condition and the functions (4.36a), (4.36b) and (4.36c) for the Dirichlet boundary condition. The effect of taking one boundary condition or the other can be observed from Figure 4.7 to Figure 4.14.

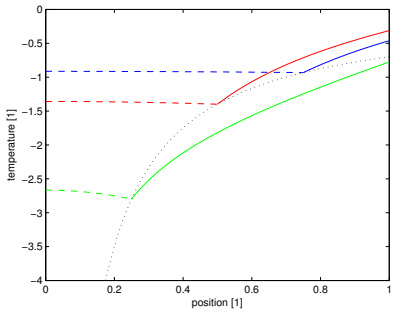

Figure 4.7: Newton BC with $R_0 = 10$ nm and $\beta = 10$.

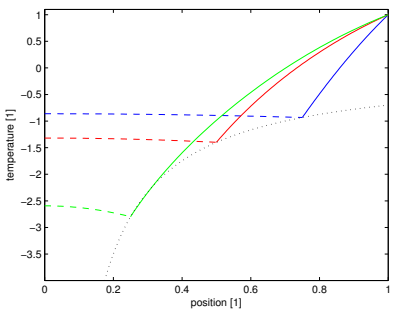

Figure 4.8: Dirichlet BC with $R_0 = 10$ nm and $\beta = 10$.

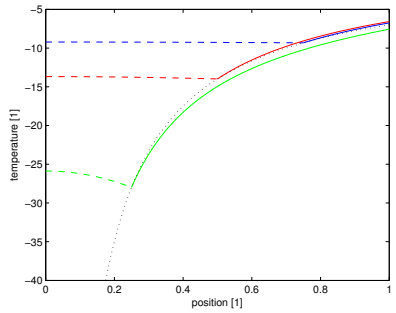

Figure 4.9: Newton BC with $R_0 = 10$ nm and $\beta = 100$.

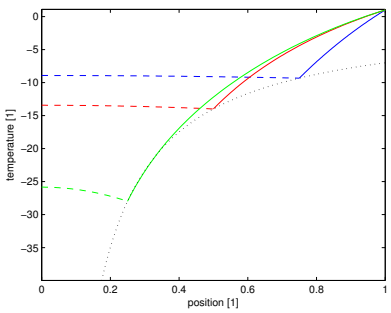

Figure 4.10: Dir. BC with $R_0 = 10$ nm and $\beta = 100$.

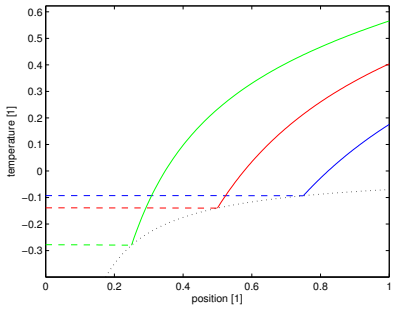

Figure 4.11: Newton BC with $R_0 = 100$ nm and $\beta = 10$.

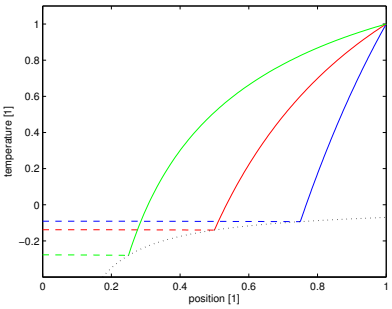

Figure 4.12: Dir. BC with $R_0 = 100$ nm and $\beta = 10$.

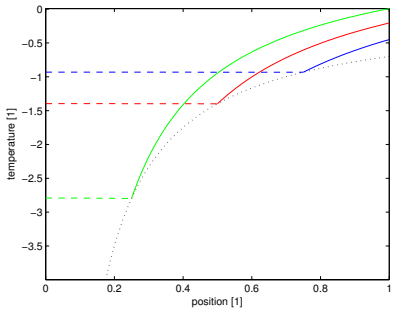

Figure 4.13: Newton BC with $R_0 = 100$ nm and $\beta = 100$.

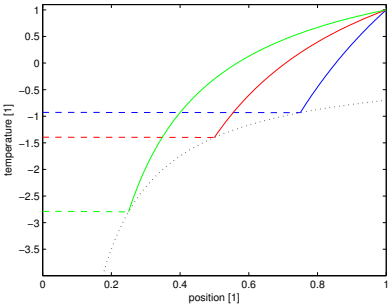

Figure 4.14: Dir. BC with $R_0 = 100$ nm and $\beta = 100$.

Imposing a Dirichlet boundary condition pins the temperature on the outer boundary to 1. Then, as the interface boundary condition is also fixed, the liquid solution is really warmer compared to imposing a Newton cooling boundary condition. The choice of the liquid boundary condition is critical and it cannot be left for mathematical convenience.
This change of liquid's temperature profile makes the heat jump at the interface bigger in all the situations and will bring lower melting times, making the process unrealistic.

Chapter 5

Melting times

In this Chapter are going to be compared the different suppositions taken in this work, using the melting times obtained in every simulation. Following the same steps taken in this work, first the different models of the effective latent heat are going to be compared, then the order of the perturbed solution for the liquid and the solid problem and finally the boundary conditions of the liquid problem. All the simulations have been run with Matlab, integrating the ODE obtained from the Stefan condition using the ode45 function of Matlab. Now the melting process can be simulated and the evolution of the moving boundary will be obtained.

5.1 Effective latent heat

Previously, in Section 2.4, has been observed that the melting depression model for the effective latent heat (2.2) is not far from considering the bulk value. The Ribera and Myers model (2.3) follows the data from Lai *et al.* but these measurements do not correspond to the definition of latent heat and provides lower values for the effective latent heat. The effects of these different models can be observed from Figure 5.1 to Figure 5.4 where it is shown the evolution of the moving boundary for different situations.

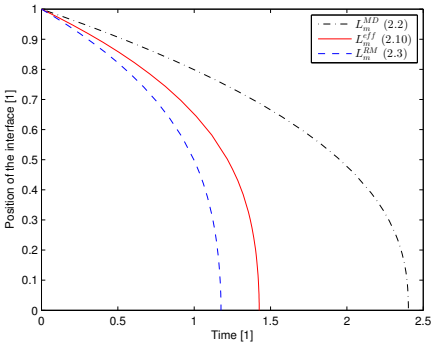

Figure 5.1: $R_0 = 10$ nm, $\beta = 10$.

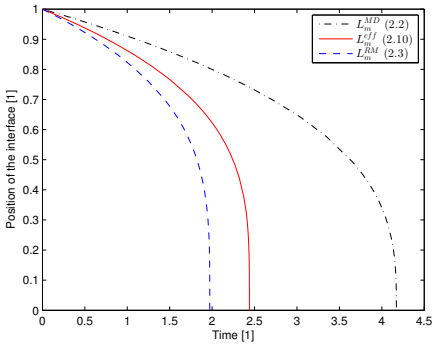

Figure 5.2: $R_0 = 10$ nm, $\beta = 100$.

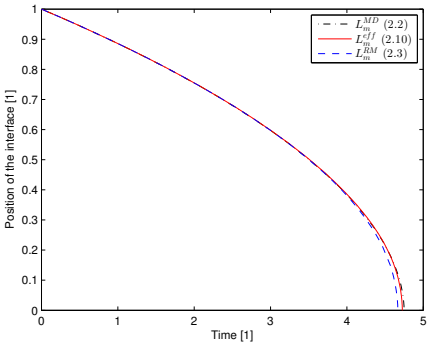

Figure 5.3: $R_0 = 100$ nm, $\beta = 10$.

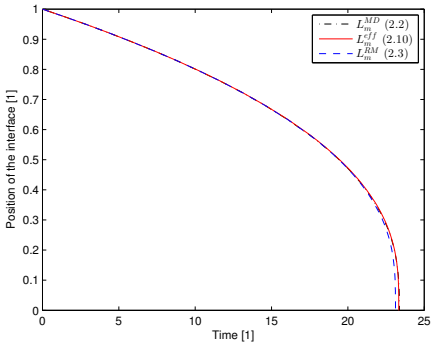

Figure 5.4: $R_0 = 100$ nm, $\beta = 100$.

It can be observed that for an initial radius of $R_0 = 100$ nm there is a small difference between models, but for $R_0 = 10$ nm the election of the model is critical. At the nanoscale, taking the bulk value for the effective latent heat brings a lot of error. This behaviour can be observed better in Figures 5.5 and 5.6, where more nanoparticle sizes have been simulated larger than 2 nm, where the continuum theory is considered to be valid [7].

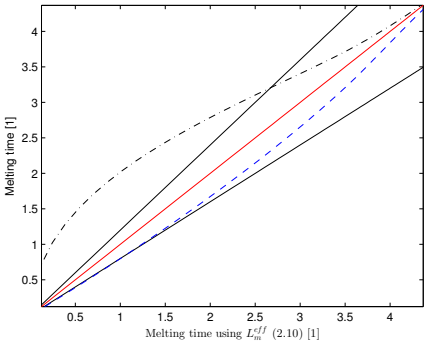

Figure 5.5: $\beta = 10$ for $R_0 \geq 2$ nm.

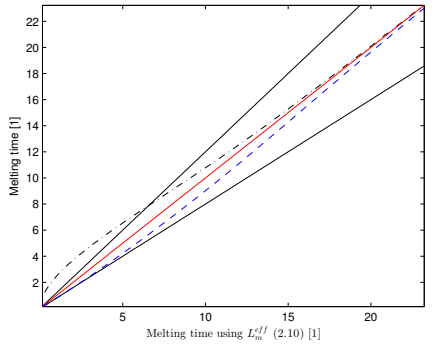

Figure 5.6: $\beta = 100$ for $R_0 \geq 2$ nm.

In Figures 5.5 and 5.6 the x-axis corresponds to the melting times obtained with the model (2.10) and the y-axis provides the melting times using the other two models (2.2) (dashed dotted line in black) and (2.3) (blue dashed line) for the same initial nanoparticle molten in the x-axis. By construction of this graph, the melting times of (2.10) model (red line) corresponds to the straight-line $y = x$. With this comparison method, it is easier to see the relative error. The black solid lines in this case correspond to a relative error of 20%.

The model proposed by Ribera and Myers (2.3) gives always lower values, on the contrary, the (2.2) model gives always higher melting times. The error grows if the nanoparticle is small and it is of the order of 20% for model (2.3). It also grows for low values of β, in other words, if the temperature of the

surroundings T_H is far from the bulk melting temperature $T_m^\star$.
This shows that the election of the expression of the effective latent heat is crucial at the nanoscale. Considering a constant effective latent heat is not accurate, but taking directly the data from Lai *et al.* can bring a relative error of 20% in the melting time.

5.2 Order of the perturbed solution

In Section (4.2) has been highlighted that if $\beta \gg 1$ the effective latent is not affected by the order of the perturbed solution. This can be observed in Figure 5.7 for $R_0 = 10$ nm and $\beta = 100$.

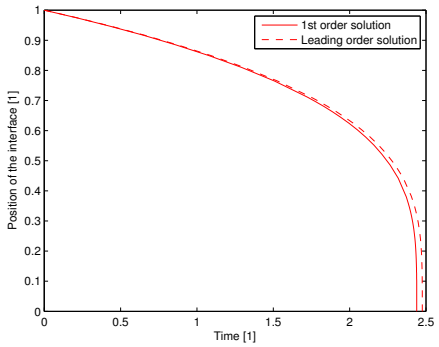

Figure 5.7: Leading order vs first order perturbed solution with $\beta = 100$ and $R_0 = 10$ nm.

Otherwise, for $\beta = 10$ the inverse of the Stefan number is not really large and there are differences between the perturbed solutions. In Section (4.2) has been stated that for the first order perturbed solution, if $k \gg 1$, a positive term is added to the effective latent heat (4.35). This implies higher melting times. This can be observed in Figure 5.8 for $R_0 = 10$ nm and $\beta = 10$.

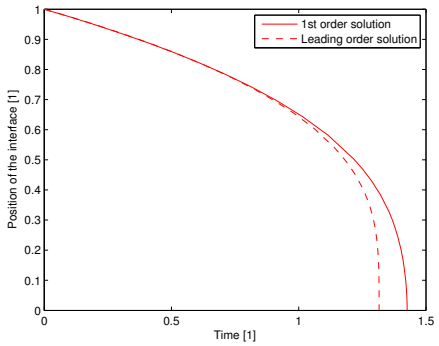

Figure 5.8: Leading order vs first order perturbed solution with $\beta = 10$ and $R_0 = 10$ nm.

The same occurs with $R_0 = 100$ nm and $\beta = 10$ in Figure 5.9.

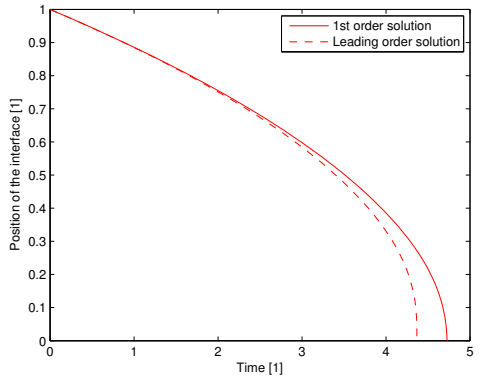

Figure 5.9: Leading order vs first order perturbed solution with $\beta = 10$ and $R_0 = 100$ nm.

Then, when $\beta = 10$, the surrounding temperature is far from the bulk melting temperature and there are more differences between the perturbed solutions. As previously in Section 5.1, more nanoparticles have been simulated with different initial radii.

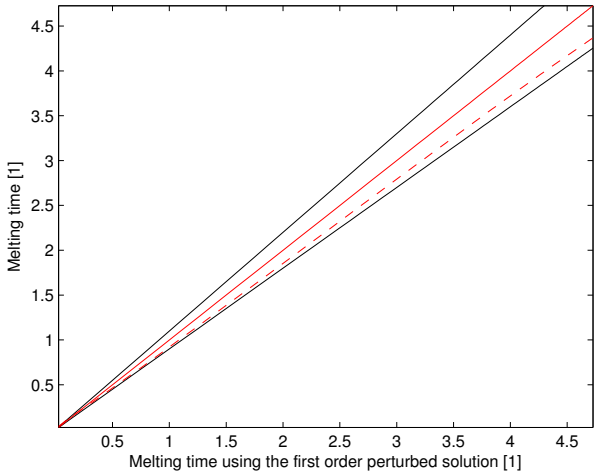

Figure 5.10: Melting times comparison with $\beta = 10$ for $R_0 \geq 2$ nm. The solid line in red corresponds to the melting times using the first order perturbed solution and the dashed line red, using the leading order. The black solid lines now correspond to a relative error of 10%.

For lower values of β, taking the leading order is not accurate and lower melting times are obtained giving a relative error of 10% for melting times.

5.3 Outer boundary condition

At this point of the work, it has been noticed that depending on the latent heat model used, a relative error of 20% can be committed, and for the perturbed solution, a relative error of 10%. For this reason, in this section is going to be used the (2.10) model for latent heat and the perturbed solution of first order for the temperature profiles. Comparing the Newton cooling condition used in this work with the Dirichlet boundary condition introduced in Chapter 4, are obtained the following melting times from Figure 5.11 to Figure 5.14.

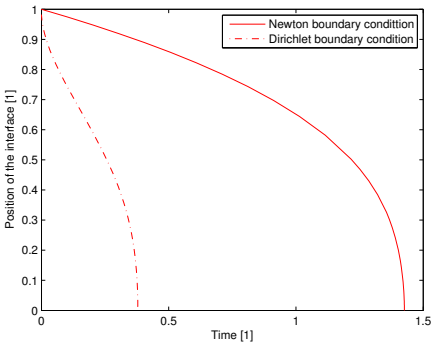

Figure 5.11: $R_0 = 10$ nm, $\beta = 10$.

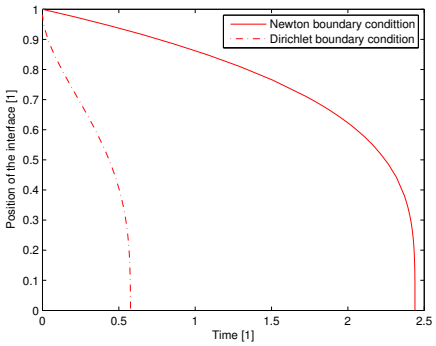

Figure 5.12: $R_0 = 10$ nm, $\beta = 100$.

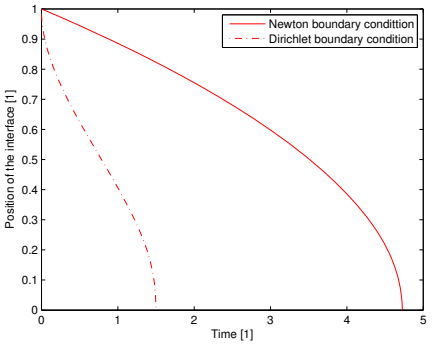

Figure 5.13: $R_0 = 100$ nm, $\beta = 10$.

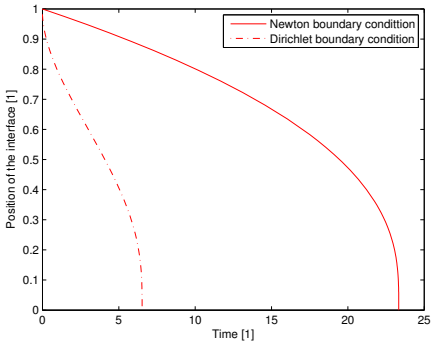

Figure 5.14: $R_0 = \beta = 100$.

In all situations it is observed that if a Dirichlet boundary condition is imposed, the melting is really faster. In addition, at the beginning of the melting, there is an infinite slope in the Dirichlet case, that physically it has no sense. Then, considering the Newton cooling boundary condition is more accurate than taking a Dirichlet boundary condition.
The consequences of taking a boundary condition or the other, can be observed in (5.15) and (5.16) where the black solid lines correspond to a relative error of 70%.

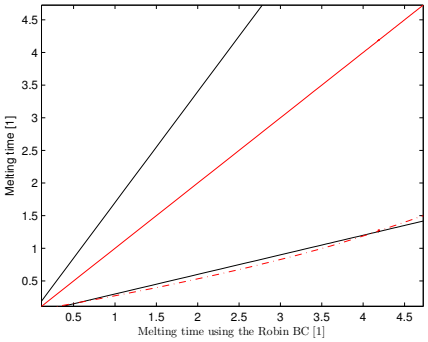

Figure 5.15: $\beta = 10$ for $R_0 \geq 2$ nm.

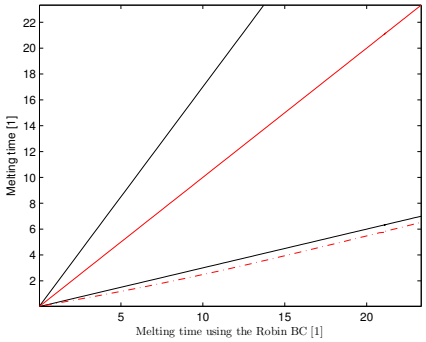

Figure 5.16: $\beta = 100$, $R_0 \geq 2$ nm.

This means that the biggest error comes from the outer boundary condition. Compared to the effective latent heat expression chosen or the order of the perturbed solution, the critical point is the election of the outer boundary condition. Imposing a Dirichlet boundary condition can bring an error of 70% independently of the size of the particle, this means that is not an error related to the nanoscale. The same occurs with the perturbed election, where the relative error does not depends on the size of the nanoparticle. Otherwise, the election of the effective latent heat depends on the initial radius of the nanoparticle and it is higher at the nanoscale.

Chapter 6

Conclusions

In this work, a study of a spherical nanoparticle has been carried out. The main differences with other studies of the Stefan problem is the use of a size-dependent latent heat and a convective boundary condition for the liquid problem. It can be concluded that (following the same items as in the Introduction):

- At the nanoscale, a new term appears into the Stefan condition, related to the energy needed to create the new surface during melting.
- At the nanoscale, the effective latent heat is not constant anymore. Some experiments show this variation but they do not correspond to the definition of latent heat. Modelling aims to explain physics phenomena, but if the data is wrong, no matter how good the model is.
- The one-phase reduction taking the solid at constant temperature is not accurate at the nanoscale. A solid profile warmer than the interface temperature is obtained that introduces a heat flux into interface.
- The two-phase reduction of the Stefan problem, taking only the leading order of the perturbed solution, gives a warmer solution in the liquid.
- Using a Dirichlet boundary condition for the liquid gives, independently of the particle size, a really warmer solution for the liquid temperature, compared to using a Robin boundary condition.
- Comparing the melting times, the biggest error (70%) comes from the choice of the outer boundary condition. An error of 20% comes from the choice of the effective latent heat model and the choice of the order of the perturbed solution gives an error of 10%. The error coming from the choice of the latent heat is the unique that is related to the nanoscale.

Putting aside the main conclusions of this work, it is observed that at the nanoscale, the classical formulation of the Stefan problem does not work because the material properties change with size. This means that, in future work, a deep study of the material properties must be done to see its relation with pressure, temperature and size.

Bibliography

[1] What is thermal evaporation? `http://www.ajaint.com/what-is-thermal-evaporation.html`. [Online; accessed 30-May-2016].

[2] V. Alexiades and A.D. Solomon. *Mathematical modeling of melting and freezing processes*. Hemisphere Publishing Corporation, Washington DC, 1st edition, 1993.

[3] R.B. Bird, W.E. Stewart, and E.N. Lightfoot. Transport phenomena. 2007.

[4] P. Buffat and J-P. Borel. Size effect on the melting temperature of gold particles. *Physical review A*, 13(6):2287, 1976.

[5] M. De Decker. Methods for solving 1d Stefan problems with application to contact melting. 2011.

[6] L.C. Evans. Partial differential equations. 2010.

[7] F. Font. Beyond the classical Stefan problem. 2014.

[8] F. Font and T.G. Myers. Spherically symmetric nanoparticle melting with a variable phase change temperature. *Journal of nanoparticle research*, 15(12):1–13, 2013.

[9] F. Font, T.G. Myers, and S.L. Mitchell. A mathematical model for nanoparticle melting with density change. *Microfluidics and Nanofluidics*, 18(2):233–243, 2015.

[10] S.L. Lai, J.Y. Guo, V. Petrova, G. Ramanath, and L.H. Allen. Size-dependent melting properties of small tin particles: nanocalorimetric measurements. *Physical review letters*, 77(1):99, 1996.

[11] T.G. Myers and F. Font. On the one-phase reduction of the Stefan problem with a variable phase change temperature. *International Communications in Heat and Mass Transfer*, 61:37–41, 2015.

[12] H. Ribera and T.G. Myers. A mathematical model for nanoparticle melting with variable latent heat and melt temperature. *Submitted to Macrofluidics and Nanofluidics*, 2016.